



## Investigation of methylene blue adsorption in wastewater using nano-zeolite modified with copper

Farhad Salimi<sup>a,\*</sup>, Mehran Eskandari<sup>a</sup>, Changiz Karami<sup>b</sup>

<sup>a</sup>Department of Chemical Engineering, Faculty of Engineering, Kermanshah Branch, Islamic Azad University, Kermanshah, Iran, Tel. +98 341 3221452; emails: f.salimi@iauksh.ac.ir (F. Salimi), mehran.eskandari2@gmail.com (M. Eskandari)

<sup>b</sup>Department of Chemistry, Faculty of Basic Science, Kermanshah Branch, Islamic Azad University, Kermanshah, Iran, email: changiz.karami@gmail.com

Received 8 December 2016; Accepted 26 July 2017

---

### ABSTRACT

In this study, the adsorption of methylene blue (MB) dye using the nano-zeolite modified with copper (Cu-zeolite) was investigated. The modified zeolite was characterized by scanning electron microscopy, Fourier transform infrared spectroscopy, X-ray powder diffraction and transmission electron microscopy. Moreover, the effect of experimental parameters such as pH, contact time and initial concentration on adsorption of dye was studied. Results indicated that the optimum conditions for maximum adsorption of 20 mg/L MB were 30 min contact time, pH = 7 and 8 g/L adsorbent; the remaining MB in the solution was 1.75%. The equilibrium data were found to be well represented by Langmuir isotherm equation and the adsorption process was described by pseudo-second-order kinetic model for MB.

*Keywords:* Adsorption; Modified nano-zeolite with copper; Methylene blue; Colored water

---

### 1. Introduction

Dye-containing wastewaters from the textile industry are one of the main pollutant sources worldwide. There are over 100,000 different textile dyes with an estimated annual production of 700,000 metric tons. Of these dyes, 30% are used in excess of 1,000 tons per annum and 90% are used at the level of 100 tons per annum [1–3]. In addition to the textile industry, the consumption of dyes has increased in cosmetics, pulp and paper, paint, pharmaceutical, food, carpet and printing industries among others. Besides coloring the wastewater, dyes and their breakdown products are toxic, carcinogenic and mutagenic to life forms, and they can cause allergies and skin diseases [4–6]. Dyes have complex aromatic structures and their removal is generally difficult. Moreover, they are usually biologically non-degradable, resistant to aerobic digestion, and are stable to light, heat and oxidizing agents [7,8]. The possible reason for non-biodegradability of these

dyes in conventional systems is the lack of necessary enzymes to biodegrade these dyes in the environment [3,9–14]. One of the best methods for wastewater treatment is adsorption. Amongst the features of adsorption, flexibility, simplicity of design and insensitivity to toxic pollutants are the most important. Activated carbon is the most popular adsorbent, and has been cited by the US Environmental Protection Agency as one of the best available control technologies [15]. The traditional technologies based on adsorption frequently involve the use of activated carbon for the removal of organic contaminants in water. However, it is well known that regeneration of active carbon is complicated [16–19], and many researchers have focused on various materials that are able to remove organic pollutants from water [20–30].

One of the important class of hydrated aluminosilicates is zeolites. They own cage-like structures with internal and external surface areas of up to several hundred square meters per gram. An important property of these materials is the capacity to be easily regenerated while retaining their initial properties. The wide use of synthetic and natural zeolites as

---

\* Corresponding author.

adsorbents for removal of phenolic compounds from water has been reported [31–34]. Zeolites are a group of crystallized hydrated aluminosilicates with fine pores containing balanced cations from earth alkaline metals group ( $\text{Na}^+$ ,  $\text{K}^+$ ,  $\text{Mg}^{2+}$  and  $\text{Ca}^{2+}$ ), which absorb water and release it reversibly. They can absorb and release water reversibly without major change in their structure and exchange some of their cations.

Copper is one of the most famous metals, which has been used for thousands of years. It is essential for all living organisms, which has lower toxicity and is cheaper than other metals. In addition, copper ions are doped in the pores of the nano-zeolite leading to their increased surface area and increased use as an adsorbent to remove organic contaminants. The main objective of the present study is to evaluate the feasibility of applying Cu-zeolite to the methylene blue (MB) removal from aqueous solutions. We focused on enhancing adsorption capacity and reducing adsorption cost of toxic MB by loading Cu ions on the synthesized nano-zeolite surface.

## 2. Materials and methods

All chemicals used in this study, such as natrolite zeolite, copper nitrate and MB were prepared from Merck Company with high purity. In this study, MB, which is an aromatic chemical compound, and water polluting dye were used.

### 2.1. Instruments

UV-Vis absorption spectra were acquired on a Cary 100 UV-Vis spectrometer (Varian, USA) at room temperature (23°C–25°C) by using a double beam. FTIR spectra were measured on a Bruker spectrophotometer pressed into KBr pellets and is reported in wave numbers ( $\text{cm}^{-1}$ ). Transmission electron microscopy (TEM) was carried out on a Zeiss-EM10C-80 KV and field emission scanning electron microscopic (FESEM) images were obtained using a HITACHI S-4160 FESEM. X-ray powder diffraction (XRD) pattern on a BRUKER B8 ADVANCE X-ray diffractometer with  $\text{CuK}\alpha$  radiation. Typically, a scanning velocity of  $1.5^\circ \cdot \text{min}^{-1}$  was used to scan the peaks of the zeolite diffraction pattern in the  $2\theta$  range between  $5^\circ$  and  $80^\circ$ . A Metrohm 692 pH meter (Herisau, Switzerland) was used for pH measurements.

### 2.2. Preparation of nano-natrolite zeolite

To prepare nano-natrolite zeolite, certain amounts, 2 g, of natrolite zeolite were placed in electric furnace at temperature  $700^\circ\text{C}$  for 6 h. Then, it was cooled to room temperature and kept in the closed container to use it [35,36].

### 2.3. Preparation of nano-zeolite modified by copper

The Cu-doped zeolite was prepared through using the following incipient wetness method. The  $\text{Cu}(\text{NO}_3)_2 \cdot 9\text{H}_2\text{O}$  (0.3 g) (99%, Merck, Germany) and natrolite zeolite were used for this purpose. Initially, 2 g of zeolite and 3 g of  $\text{Cu}(\text{NO}_3)_2 \cdot 9\text{H}_2\text{O}$  were mixed and stirred for 2 h at room temperature until a uniform solution was formed. Then, the solution was heated to  $700^\circ\text{C}$  for 6 h with  $2^\circ\text{C} \cdot \text{min}^{-1}$  heating rate. The Cu-zeolite was washed with distilled water several times, isolated using a centrifuge and ultimately, dried in an oven (at  $120^\circ\text{C}$  for 12 h) [35,36].

### 2.4. Procedure

For performing a typical removal experiment, 0.04 g of raw natrolite zeolite, nano-zeolite or Cu-zeolite powder was mixed with 10 mL of MB solution at 20 ppm concentration. The suspension was shaken at 200 rpm for 30 min at room temperature and then centrifuged at 4,000 rpm for 10 min. Finally, the adsorption amount of the obtained solution was taken using UV/Vis. The effect of various parameters such as initial MB concentration, contact time, pH, temperature, etc. was studied on the removal extent of MB [37].

The amount of MB adsorbed onto Cu-zeolite and the removal efficiency were calculated by the following equations:

$$q_t = \frac{(C_0 - C_e)V}{m} \quad (1)$$

$$\text{Removal efficiency (\%)} = (C_0 - C_f)/C_0 \times 100 \quad (2)$$

where  $C_0$ ,  $C_f$  and  $C_e$  ( $\text{mg L}^{-1}$ ) are the initial, final and equilibrium concentrations of contaminants, respectively.  $q_t$  ( $\text{mg g}^{-1}$ ) is the adsorbed amount of adsorbate per unit mass of the adsorbent at time  $t$ .  $V$  (L) is the volume of adsorption solution and  $m$  (g) is the mass of adsorbent [38].

## 3. Results and discussion

### 3.1. Investigating the structure of adsorbents

The structures of the as-prepared products were first characterized by scanning electron microscopy (SEM) and TEM. Fig. 1 presents the SEM images of the zeolite and Cu-zeolite, which exclusively show a large number of nanoparticles. Fig. 2 shows a TEM image of the zeolite and Cu-zeolite. The cores of the Cu have a typical size of less than 100 nm, but the bulk of the nano-zeolite particles contains aggregates with no fractal features and a uniform size.

### 3.2. Investigating the structure of adsorbents using XRD pattern

XRD pattern results are shown in Figs. 3 and 4. The results indicate that main peaks related to the Cu-zeolite samples match the standard sample. Also, comparing these two figures indicates that a series of peaks at 35.74, 38.95 and  $50.04^\circ$  are shown which confirm the formation of CuO nanoparticles. Using this evidence, it can be realized that copper is present in the structure of nano-zeolite. The initial peak that has extremely increased indicates anisotropic crystallographic nature of this sample and placement of particles is beside each other [39,40].

In this sample, no impure peak was seen. In addition, by using the Scherrer equation, the peak of  $19^\circ$  (111) is shown and the mean of particle size is about 12 nm [41,42].

### 3.3. Investigation of adsorbents' structure using FTIR

Fourier transform infrared spectroscopy (FTIR) spectra of nano-zeolite are shown in Fig. 5. The peak in the areas of 1,450, 638, 677, 769, 1,036 and  $1,645 \text{ cm}^{-1}$  represents a link related to nano-zeolite. In addition, the peak in the area of

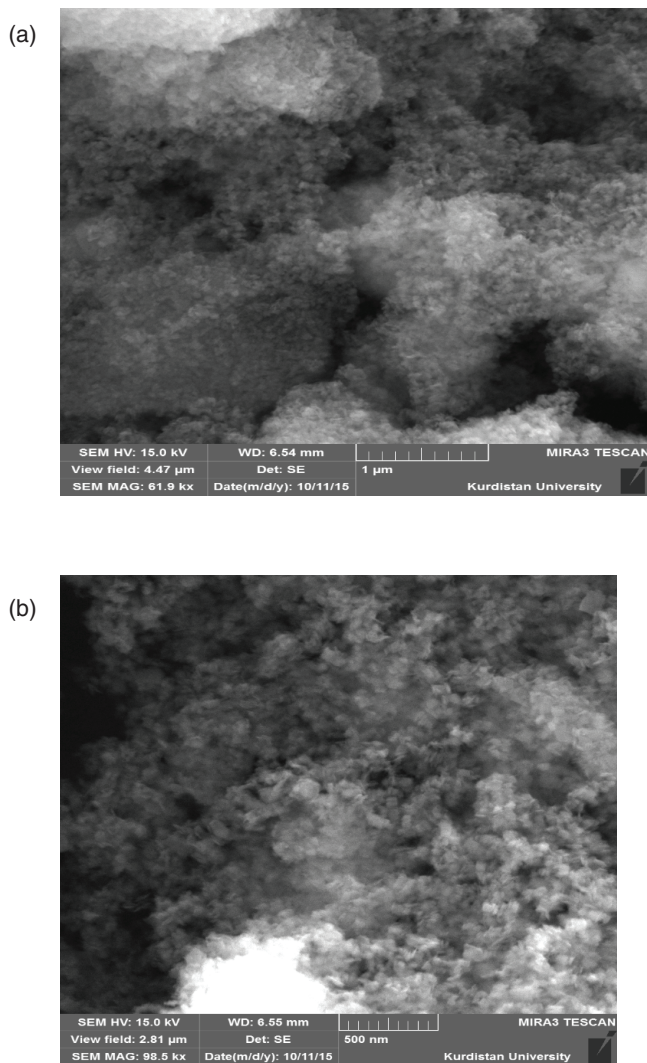


Fig. 1. SEM image for nano-zeolite absorbent (a) and Cu-zeolite (b).

$3437.02\text{ cm}^{-1}$  is related to stretching vibrations in OH ions of the peak in endcylan groups, and the peak in the area of  $769$  and  $1,036\text{ cm}^{-1}$  is related to Si-O and Al-O, respectively [43,44]. Fig. 6, related to Cu-zeolite, is similar to Fig. 5; however, the peak in the area of  $634\text{ cm}^{-1}$  is related to copper, which represents the presence of copper in the compound. The results of the powder XRD pattern and framework FTIR spectra clearly indicate that the modification by ion-exchange technique does not change in framework composition natrolite zeolite, phase purity and crystallinity of parent NaX and its exchanged forms [45–47].

#### 3.4. Investigating the effect of pH on removal efficiency

One of the important experimental parameter in removal extent of pollutants is solution pH because of its effects on the surface charge of the sorbent and ionic forms of MB present in solution. The optimum pH for the adsorption of MB was found to be in the range 8–12 (Fig. 7). This can be explained with the electrostatic interaction of MB (because of its cationic structure) with negatively charged surface of the modified

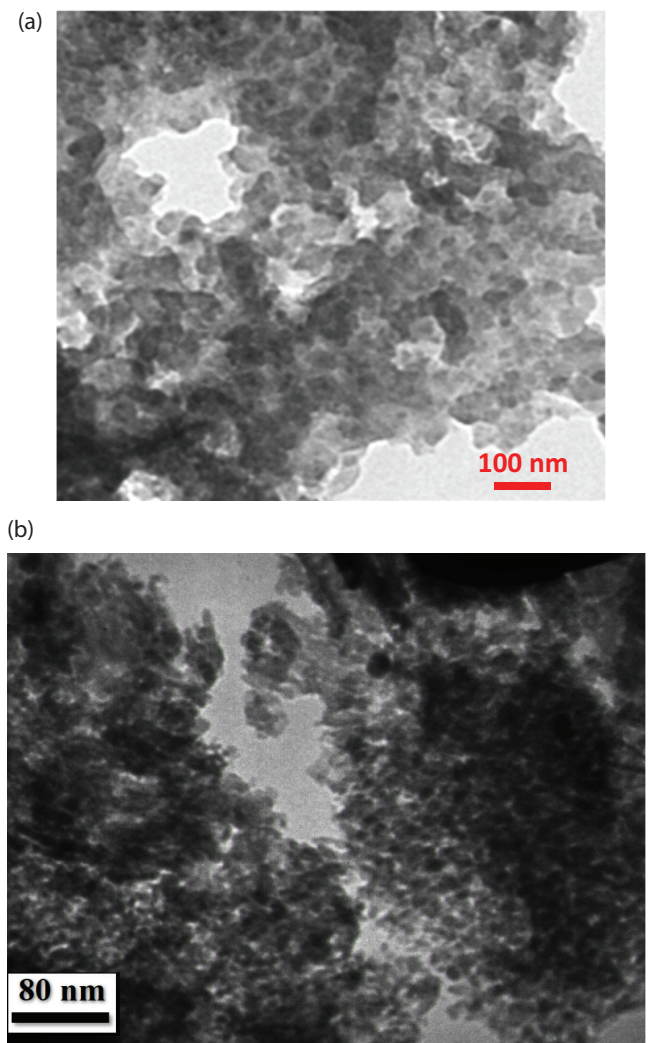


Fig. 2. TEM photography for nano-zeolite absorbent (a) and Cu-zeolite (b).

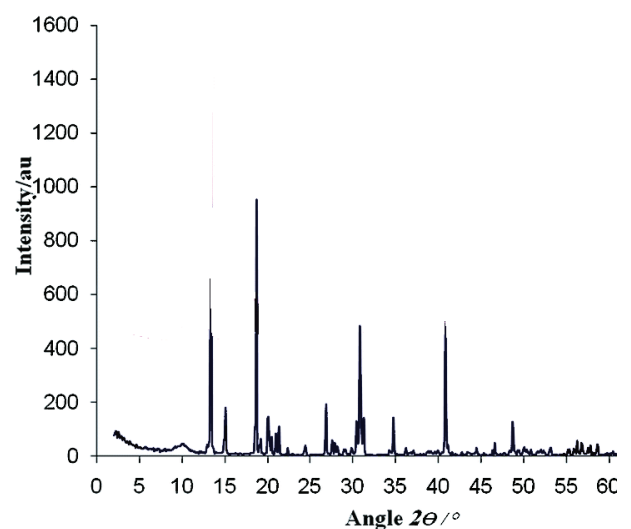


Fig. 3. XRD image to nano-zeolite.

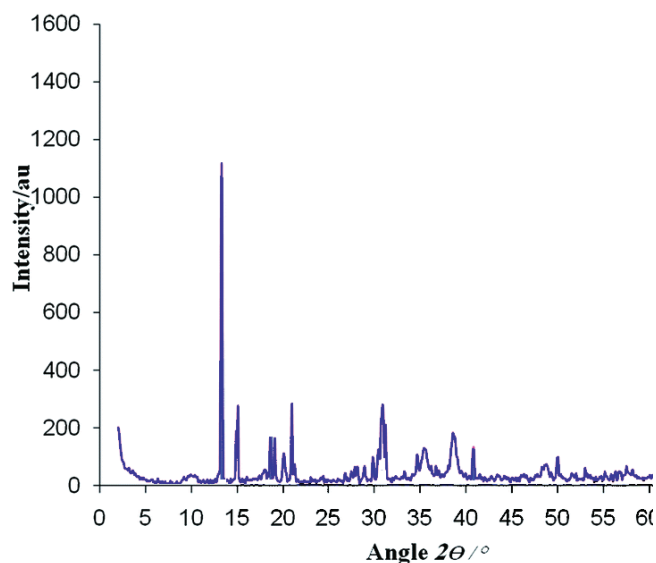


Fig. 4. XRD pattern to Cu-zeolite.

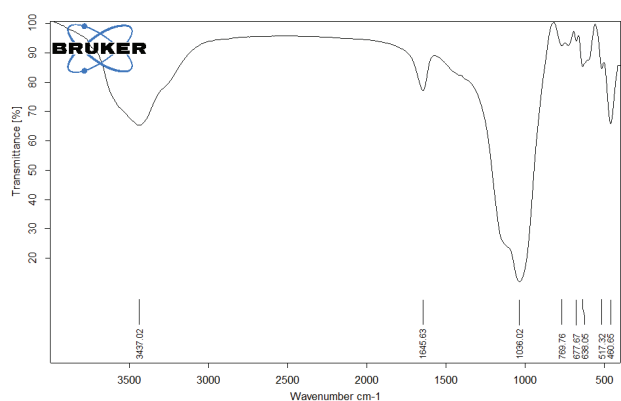


Fig. 5. FTIR spectra of nano-zeolite.

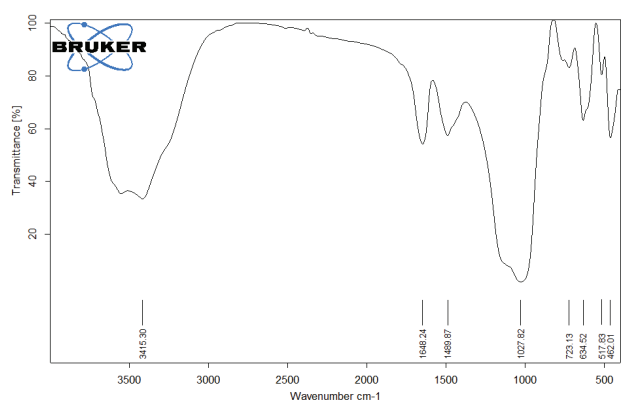


Fig. 6. FTIR spectra of Cu-zeolite.

nano-zeolite. The pH of point of zero charge of the sorbent,  $\text{pH}_{\text{PZC}}$ , was 8 [48]. At lower pH ( $\text{pH} < \text{pH}_{\text{PZC}}$ ), the adsorbent has positive charge. Also MB may be present in its cationic form via protonation of its sulfur or nitrogen atoms. Hence, repulsive force between such cationic form and positively charged

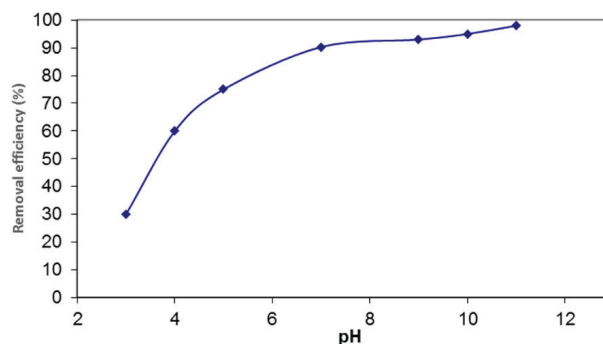


Fig. 7. Effect of pH on adsorption of dye (conditions: 8 mg adsorbent, 10 mL of 20 mg/L of cationic dyes duration of oscillation time of 20 min).

sorbent repels MB from the adsorbent surface. In addition, ion exchange of protons with Cu(II) cation in zeolite, decrease Cu(II) extent of zeolite as complexing agents for removing MB. In such conditions, protonated MB molecules have little tendency with remained Cu(II) on the zeolite. By increasing the pH ( $\text{pH} \geq \text{pH}_{\text{PZC}}$ ), these problems tend to decrease and removal extent tends to increase, so the best MB removal was obtained at pH 8 and thereafter no significant increase was observed [49]. Similar trends were observed for the adsorption of MB onto Fe(III)/Cr(III) hydroxide [50], malachite green onto agro-industry waste [51], MB on zeolite [52,53], MB onto various carbons [54] and MB onto elaeagnus gastifolial [55].

### 3.5. Investigating the effect of adsorbent rate on the removal efficiency

At this stage, the adsorption rate of the adsorbent sample on the removal of the dye was examined. For this purpose, at the optimal pH equal to 7, various weights of adsorbent were used for MB solution at concentration of 20 ppm. In each test, adsorbent sample was contacted with 10 mL of the dye samples for 20 min. Results are shown in Fig. 8. As the results indicate, when the amount of the adsorbent increases from 0.04 to 0.1 g, an increase is also seen in the percentage of removal of the dye. According to the experiments, the optimal mass for the adsorbent is 0.08 g. In general, the adsorbent's capacity to adsorb the dye increases with increased adsorbent mass, because increased mass of adsorbent is associated with increased specific surface area and adsorption sites. In addition, as the amount of the adsorbent increase, no change is seen in the percentage of removal of the dye, since the surface sites are filled and saturated.

### 3.6. Investigating the effect of reaction time on removal efficiency

This test was performed within 5–30 min with the change range of 5 min and the optimal time was accordingly obtained. Results of Fig. 9 show that by increasing the contact time, removal efficiency increases and reaches its optimal time at 20 min and the removal percentage reaches to 98.32 and after that the increase in the percentage of removal efficiency have been insignificant. Also, the increased contact time leads to increased MB adsorption by surface sites (vacant surface sites) on the surface of the adsorbent.

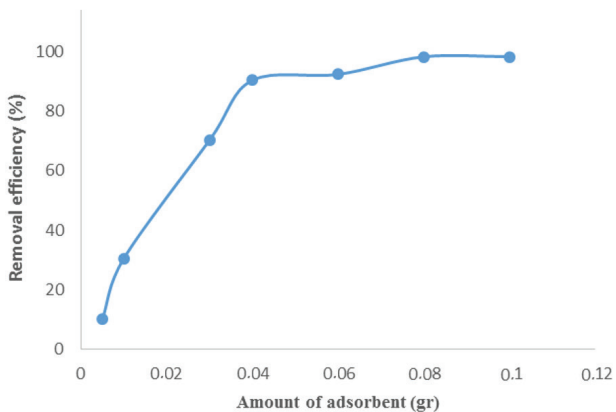


Fig. 8. Effect of amount of adsorbent on adsorption of dyes (conditions: pH = 7.0 and 10 mL of 20 mg/L of cationic dyes duration of oscillation time of 20 min).

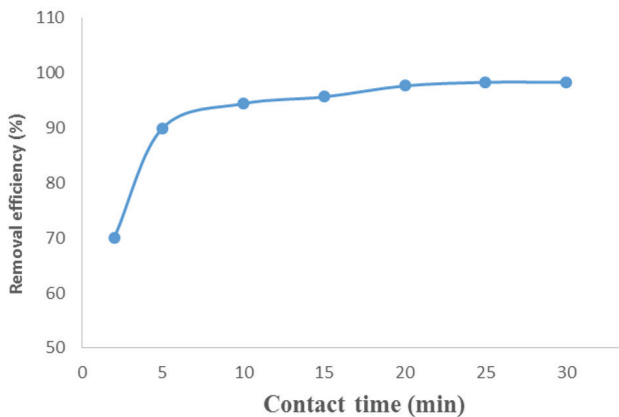


Fig. 9. Effect of contact time on dye adsorption (conditions: 10 mL of 20 mg/L of dyes, pH = 7.0 and 80 mg adsorbent).

### 3.7. Investigating the effect of reaction temperature on removal efficiency

In Fig. 10, the effect of contact time of adsorbent on adsorption of MB is shown. Results showed that the MB adsorption had the highest dye removal by Cu-zeolite at a pH of 7 and 0.08 g of the adsorbent and MB with the concentration of 20 ppm in 20 min at the room temperature (25°C). As the temperature rises, the percentage of dye removal decreases, since the MB molecules move more and their adsorption by the surface reduces.

As the temperature rises, the percentage of dye removal decreases, since the MB molecules move more and their adsorption by the surface reduces [56].

### 3.8. Investigating the effect of dye solution concentration of methylene blue on adsorption efficiency

Fig. 11 shows the effect of the initial MB concentration on its surface adsorption by the adsorbent. To perform this test, the parameters of time, adsorbent mass and pH on optimum values were regulated (0.08 g of adsorbent, 20 min contact time and pH = 7). As shown in the figure, the rate of

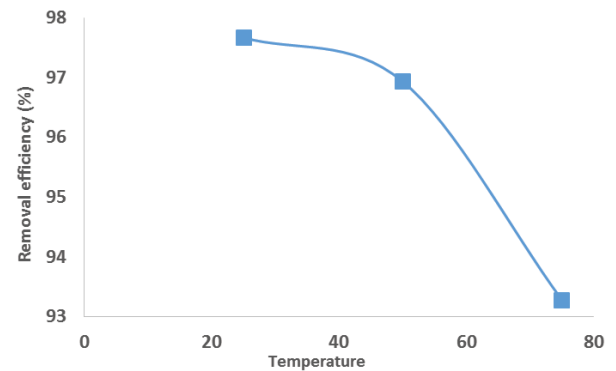


Fig. 10. Effect of temperatures on adsorption of dyes (conditions: 10 mL of 20 mg/L of dyes, pH = 7.0 and 80 mg adsorbent).

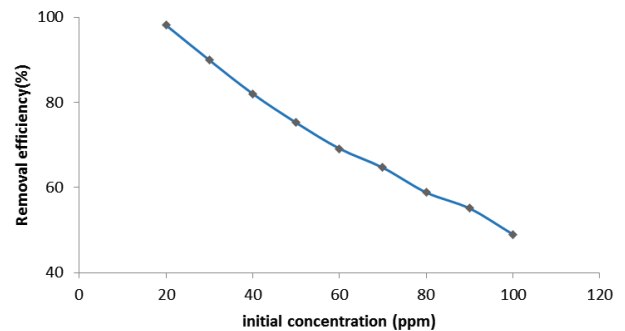


Fig. 11. Effect of initial dye concentration on adsorption of dyes (conditions: 10 mL of dyes, pH = 7.0 and 80 mg adsorbent).

the absorbed dye was reduced; thus, it can be stated that dye removal is influenced by dye initial concentration. At low concentrations, MB was adsorbed on the vacant positions of adsorbent surface and these places were saturated and filled by increasing the concentration. When the initial MB dye concentration was low, there were very high number of sites available for dye adsorption on the surface of the adsorbent. However, as long as the initial MB dye concentration increases, the number of moles of the MB dye is higher than the number of its vacant positions. Therefore, the available sites are quickly saturated and dye removal rate decreases.

For example, when the initial concentration of dye increases from 20 to 100 ppm, the dye adsorption rate also decreases from 98.135 to 49.01.

### 3.9. Comparison of methylene blue dye rate between natrolite zeolite, nano-zeolite and Cu-zeolite

By comparing zeolite, nano-zeolite and Cu-zeolite adsorbents, the efficiency of MB removal significantly increases if the nano-zeolite modified by copper was used as the adsorbent.

In summary, the objectives of using Cu-zeolite include:

- reduced reaction time
- reduced adsorbent amount and
- increasing the amount of methylene blue adsorption

The information presented in Table 1 displays the results of removing MB from the solution.

Adsorbent efficiency: Cu–zeolite > nano-zeolite > zeolite.

### 3.10. Adsorption isotherm

Adsorption isotherm describes how the adsorbent interacts with the adsorbed substance. Isotherms of Langmuir and Freundlich were used for evaluating the parameters such as adsorption capacity and adsorption mechanism.

Langmuir considered adsorption as an ideal adsorption on an ideal surface. This model assumes that adsorption can only be done at constant sites and can only maintain one adsorbing molecule at a time (single-layered) [57,58]. All the sites are equivalent and there is no interference between the adsorbed molecule and the adsorption site. The Langmuir equation has been derived from Gibbs' method, which has been shown in Eq. (3). In which,  $q_{max}$  (mg/g) is the monolayer adsorption capacity,  $b$  (L/g) is the Langmuir constant that is related to the free energy of adsorption, while  $C_e$  (mg/L) is the equilibrium concentration of adsorbate in solution and  $q_e$  (mg/g) is the concentration of adsorbate on the surface of adsorber.

Eq. 3 has been shown as follows:

$$\frac{C_e}{q_e} = \frac{C_e}{q_{max}} + \frac{1}{b \cdot q_{max}} \quad (3)$$

The essential characteristics of Langmuir isotherm can be explained using a dimensionless constant,  $R_L$ , known as separation factor, which is calculated using the following equation:

$$R_L = \frac{1}{(1 + bC_0)} \quad (4)$$

where  $C_0$  (mg L<sup>-1</sup>) is the initial dye concentration and  $b$  is the Langmuir adsorption constant (L mg<sup>-1</sup>). The  $R_L$  value describes adsorption process to be unfavorable ( $R_L > 1$ ), linear ( $R_L = 1$ ), favorable ( $0 < R_L < 1$ ) or irreversible ( $R_L = 0$ ) [58].

The laboratory data was applied to the equation above and the graph  $C_e/q_e$  was obtained based on the linear regression  $C_e$ . The second model is the Freundlich isotherm and it is a multi-site adsorption isotherm for heterogeneity surfaces [59] and its total form has been shown in the following equation:

$$\ln q_e = \ln K_f + \frac{1}{n} \ln C_e \quad (5)$$

In which,  $q_e$  and  $C_e$  are the parameters in Eq. (3) and  $K_f$  and  $n$  are Freundlich parameters related to the extent of adsorption and the intensity of adsorption, respectively.

A linear graph of  $q_e$  based on  $\ln C_e$  shows that the Freundlich model describes the adsorption process in the best way possible. Comparing  $R^2$  values evidently indicated that the Langmuir model possessed the best fit with the experimental equilibrium data (Table 2) [49,60,61]. This suggests that the MB was adsorbed in the form of monolayer coverage onto the surface of adsorbent. In addition, the obtained value of  $n$  ( $4.48 > 1$ ) corresponds to a favorable adsorption process. On the other hand, the  $R_L$  value of MB obtained from Langmuir isotherm lied at 0.0211, which indicated that the adsorption was favorable and in consistence with the Freundlich model [62].

### 3.11. Kinetic studies

Adsorption kinetics was studied to obtain the mechanism of heavy metal ions adsorption, as well as the time needed to reach equilibrium and the potential rate-controlling steps, such as mass transport and chemical reaction processes [57,63].

Laboratory data were fitted with Lagergren pseudo-first-order kinetic [64] and Ho pseudo-second-order kinetic [65]. This was done for molecular reviewing of the adsorption mechanism and the stages controlling its speed. The Lagergren pseudo-first-order kinetic and Ho [65] pseudo-second-order kinetic models have been, respectively, presented in Table 3.

The information presented in this table indicated how the contact time affects the adsorption process at different times. The adsorption behavior showed that the adsorption system best fits the pseudo-second-order ( $R^2 = 0.9988$ ) model, illustrating that the rate-limiting step can be chemical adsorption or chemisorption involving valence forces through sharing or exchange of electrons between the adsorbent and adsorbate [49,64]. It is by reviewing the results of this section that a multi-layer adsorption can be concluded (Table 4). In the pseudo-first-order model,  $K_1 = 0.0417$ , whereas in the pseudo-second-order model,  $K_2 = 0.53$ .

## 4. Conclusion

In this study, the MB dye adsorption using the nano-zeolite modified with copper was investigated and the following results were obtained:

Table 1

Comparing different adsorbents for methylene blue removal (conditions:  $T = 25^\circ\text{C}$ ,  $\text{pH} = 7$ , 8 mg adsorbent, 10 mL of 20 mg/L of cationic dye duration of oscillation time of 20 min)

Absorbents	% Removal
Cu–zeolite	98.32
Nano-zeolite	79.5
natrolite zeolite	60.25

Table 2

Results of the Langmuir and Freundlich models

Model	
Freundlich	Langmuir
$R^2 = 0.7451$	$R^2 = 0.8506$
$n = 4.48$	$b = 2.32$
$K_f = 1.6$	$q_{max} = 4.83 \text{ mg g}^{-1}$

Table 3  
Synthetic models of adsorption

Parameters	Equation	Kinetic models
$q_e$ : The amounts of Ag(I) ions adsorbed on the nanocomposite at equilibrium time (mg/g)	$\ln(q_e - q_t) = \ln(q_e) - K_1 t$	Pseudo-first-order
$q_t$ : The amounts of Ag(I) ions adsorbed on the nanocomposite at time $t$ (mg/g)		
$K_1$ : The first-order adsorption rate constant ( $\text{min}^{-1}$ )	$\frac{t}{q_t} = \frac{1}{K_2(q_e)^2} + \frac{t}{q_e}$	Pseudo-second-order
$K_2$ : The pseudo-second-order adsorption rate constant ( $\text{g mg}^{-1} \text{min}^{-1}$ )		

Table 4  
Lagergren pseudo-first-order kinetic and pseudo-second-order kinetic data

Order	Pseudo-second-order	Pseudo-first-order
$R^2$	0.9999	0.8904
$K$	$0.53 \text{ g mg}^{-1} \text{ min}^{-1}$	$0.0417 \text{ min}^{-1}$

- The structure of the adsorbents constructed by SEM, TEM, XRD and FTIR analyses were identified.
- The effect of operational parameters such as pH, contact time, adsorbent rate and initial concentration and temperature was examined. Results showed that the removal of dye increased by increasing contact time, adsorbent amount and pH.
- The kinetics and isotherm adsorption data were well described by the pseudo-second-order model and the Freundlich isotherm model, respectively.
- Finally, the results indicated that nano-zeolite modified with copper was a good candidate to remove cationic dye (MB) from wastewater.

#### Acknowledgment

We are thankful to Islamic Azad University Kermanshah Branch, Kermanshah, Iran, for the support of this work.

#### References

- [1] A. Baban, A. Yediler, N.K. Ciliz, Integrated water management and CP implementation for wool and textile blend processes, *CLEAN Soil Air Water*, 38 (2010) 84–90.
- [2] N. Balasubramanian, Electrochemical degradation of remazol Black B dye effluent, *CLEAN Soil Air Water*, 37 (2009) 889–900.
- [3] C. Pearce, J. Lloyd, J. Guthrie, The removal of colour from textile wastewater using whole bacterial cells: a review, *Dyes Pigm.*, 58 (2003) 179–196.
- [4] C. Zaharia, D. Suteu, A. Muresan, R. Muresan, A. Popescu, Textile wastewater treatment by homogenous oxidation with hydrogen peroxide, *Environ. Eng. Manage. J.*, 8 (2009) 1359–1369.
- [5] S. Chatterjee, D.S. Lee, M.W. Lee, S.H. Woo, Congo red adsorption from aqueous solutions by using chitosan hydrogel beads impregnated with nonionic or anionic surfactant, *Bioresour. Technol.*, 100 (2009) 3862–3868.
- [6] S. Chatterjee, M.W. Lee, S.H. Woo, Adsorption of congo red by chitosan hydrogel beads impregnated with carbon nanotubes, *Bioresour. Technol.*, 101 (2010) 1800–1806.
- [7] Q. Sun, L. Yang, The adsorption of basic dyes from aqueous solution on modified peat–resin particle, *Water Res.*, 37 (2003) 1535–1544.
- [8] M. Ravi Kumar, T. Rajakala Sridhari, K. Durga Bhavani, P.K. Dutta, Trends in color removal from textile mill effluents, *Colourage*, 45 (1998) 25–34.
- [9] S. Akhtar, A.A. Khan, Q. Husain, Potential of immobilized bitter melon (*Momordica charantia*) peroxidases in the decolorization and removal of textile dyes from polluted wastewater and dyeing effluent, *Chemosphere*, 60 (2005) 291–301.
- [10] N. Daneshvar, D. Salari, A. Khataee, Photocatalytic degradation of azo dye acid red 14 in water on ZnO as an alternative catalyst to  $\text{TiO}_2$ , *J. Photochem. Photobiol., A*, 162 (2004) 317–322.
- [11] A.R. Dinçer, Y. Güneş, N. Karakaya, Coal-based bottom ash (CBBA) waste material as adsorbent for removal of textile dyestuffs from aqueous solution, *J. Hazard. Mater.*, 141 (2007) 529–535.
- [12] S. Kansal, M. Singh, D. Sud, Studies on photodegradation of two commercial dyes in aqueous phase using different photocatalysts, *J. Hazard. Mater.*, 141 (2007) 581–590.
- [13] T. Robinson, G. McMullan, R. Marchant, P. Nigam, Remediation of dyes in textile effluent: a critical review on current treatment technologies with a proposed alternative, *Bioresour. Technol.*, 77 (2001) 247–255.
- [14] N. Azbar, T. Yonar, K. Kestioglu, Comparison of various advanced oxidation processes and chemical treatment methods for COD and color removal from a polyester and acetate fiber dyeing effluent, *Chemosphere*, 55 (2004) 35–43.
- [15] D. Suteu, C. Zaharia, T. Malutan, Biosorbents Based on Lignin Used in Biosorption Processes from Wastewater Treatment. A Review, *Lignin: Properties and Applications in Biotechnology and Bioenergy*, Nova Science Publishers Inc., New York, 2011, pp. 279–305.
- [16] J.M. Dias, M.C. Alvim-Ferraz, M.F. Almeida, J. Rivera-Utrilla, M. Sánchez-Polo, Waste materials for activated carbon preparation and its use in aqueous-phase treatment: a review, *J. Environ. Manage.*, 85 (2007) 833–846.
- [17] B. Zhang, F. Li, T. Wu, D. Sun, Y. Li, Adsorption of p-nitrophenol from aqueous solutions using nanographite oxide, *Colloid Surf., A*, 464 (2015) 78–88.
- [18] V.M. Monsalvo, A.F. Mohedano, J.J. Rodriguez, Activated carbons from sewage sludge: application to aqueous-phase adsorption of 4-chlorophenol, *Desalination*, 277 (2011) 377–382.
- [19] M. Ahmaruzzaman, Adsorption of phenolic compounds on low-cost adsorbents: a review, *Adv. Colloid Interface Sci.*, 143 (2008) 48–67.
- [20] G. Xue, M. Gao, Z. Gu, Z. Luo, Z. Hu, The removal of p-nitrophenol from aqueous solutions by adsorption using gemini surfactants modified montmorillonites, *Chem. Eng. J.*, 218 (2013) 223–231.
- [21] C.P. Goh, C.E. Seng, A.N.A. Sujari, P.E. Lim, Performance of sequencing batch biofilm and sequencing batch reactors in simultaneous p-nitrophenol and nitrogen removal, *Environ. Technol.*, 30 (2009) 725–736.
- [22] G. Buitrón, I. Moreno-Andrade, Biodegradation kinetics of a mixture of phenols in a sequencing batch moving bed biofilm reactor under starvation and shock loads, *J. Chem. Technol. Biotechnol.*, 86 (2011) 669–674.

- [23] S. Hussain, J. van Leeuwen, C. Chow, S. Beecham, M. Kamruzzaman, D. Wang, M. Drikas, R. Aryal, Removal of organic contaminants from river and reservoir waters by three different aluminum-based metal salts: coagulation adsorption and kinetics studies, *Chem. Eng. J.*, 225 (2013) 394–405.
- [24] J. Kim, F. Martinez, I. Metcalfe, The beneficial role of use of ultrasound in heterogeneous Fenton-like system over supported copper catalysts for degradation of p-chlorophenol, *Catal. Today*, 124 (2007) 224–231.
- [25] A. Nezamzadeh-Ejhieh, Z. Banan, A comparison between the efficiency of CdS nanoparticles/zeolite A and CdO/zeolite A as catalysts in photodecolorization of crystal violet, *Desalination*, 279 (2011) 146–151.
- [26] A. Nezamzadeh-Ejhieh, M. Khorsandi, A comparison between the heterogeneous photodecolorization of an azo dye using Ni/P zeolite and NiS/P zeolite catalysts, *Iran. J. Catal.*, 1 (2011) 99–104.
- [27] A. Bagheri Ghomi, V. Ashayeri, Photocatalytic efficiency of  $\text{CuFe}_2\text{O}_4$  by supporting on clinoptilolite in the decolorization of acid red 206 aqueous solutions, *Iran. J. Catal.*, 2 (2012) 135–140.
- [28] S. Mousavi-Mortazavi, A. Nezamzadeh-Ejhieh, Supported iron oxide onto an Iranian clinoptilolite as a heterogeneous catalyst for photodegradation of furfural in a wastewater sample, *Desal. Wat. Treat.*, 57 (2016) 10802–10814.
- [29] Z.-A. Mirian, A. Nezamzadeh-Ejhieh, Removal of phenol content of an industrial wastewater via a heterogeneous photodegradation process using supported FeO onto nanoparticles of Iranian clinoptilolite, *Desal. Wat. Treat.*, 57 (2016) 16483–16494.
- [30] A. Nezamzadeh-Ejhieh, M. Bahrami, Investigation of the photocatalytic activity of supported ZnO–TiO<sub>2</sub> on clinoptilolite nano-particles towards photodegradation of wastewater-contained phenol, *Desal. Wat. Treat.*, 55 (2015) 1096–1104.
- [31] L. Gómez-Hortigüela, A.B. Pinar, J. Pérez-Pariente, T. Sani, Y. Chebude, I. Díaz, Ion-exchange in natural zeolite stilbite and significance in defluorination ability, *Microporous Mesoporous Mater.*, 193 (2014) 93–102.
- [32] E. Mahmoud, R.F. Lobo, Recent advances in zeolite science based on advance characterization techniques, *Microporous Mesoporous Mater.*, 189 (2014) 97–106.
- [33] Y. Nakasaka, T. Okamura, H. Konno, T. Tago, T. Masuda, Crystal size of MFI-type zeolites for catalytic cracking of n-hexane under reaction-control conditions, *Microporous Mesoporous Mater.*, 182 (2013) 244–249.
- [34] S. Cao, F. Kang, X. Yang, Z. Zhen, H. Liu, R. Chen, Y. Wei, Influence of Al substitution on magnetism and adsorption properties of hematite, *J. Solid State Chem.*, 228 (2015) 82–89.
- [35] M. Feyzi, G. Khajavi, Investigation of biodiesel production using modified strontium nanocatalysts supported on the ZSM-5 zeolite, *Ind. Crops Prod.*, 58 (2014) 298–304.
- [36] M. Feyzi, M.M. Khodaei, J. Shahmoradi, Preparation and characterization of promoted Fe–Mn/ZSM-5 nano catalysts for CO hydrogenation, *Int. J. Hydrogen Energy*, 40 (2015) 14816–14825.
- [37] A. Naghash, A. Nezamzadeh-Ejhieh, Comparison of the efficiency of modified clinoptilolite with HDTMA and HDP surfactants for the removal of phosphate in aqueous solutions, *J. Ind. Eng. Chem.*, 31 (2015) 185–191.
- [38] L. Cui, Y. Wang, L. Gao, L. Hu, L. Yan, Q. Wei, B. Du, EDTA functionalized magnetic graphene oxide for removal of Pb (II), Hg (II) and Cu (II) in water treatment: adsorption mechanism and separation property, *Chem. Eng. J.*, 281 (2015) 1–10.
- [39] M. Nosuhi, A. Nezamzadeh-Ejhieh, High catalytic activity of Fe (II)-clinoptilolite nanoparticules for indirect voltammetric determination of dichromate: experimental design by response surface methodology (RSM), *Electrochim. Acta*, 223 (2017) 47–62.
- [40] M. Bordbar, S. Forghani-POilerood, A. Yeganeh-Faal, Enhanced photocatalytic activity of sonochemical derived ZnO via the co-doping process, *Iran. J. Catal.*, 6 (2016) 415–421.
- [41] M. Abrishamkar, A. Izadi, Nano-ZSM-5 zeolite: synthesis and application to electrocatalytic oxidation of ethanol, *Microporous Mesoporous Mater.*, 180 (2013) 56–60.
- [42] A. Mosayebi, R. Abedini, Partial oxidation of butane to syngas using nano-structure Ni/zeolite catalysts, *J. Ind. Eng. Chem.*, 20 (2014) 1542–1548.
- [43] Y.H. Lee, S.G. Pavlostathis, Decolorization and toxicity of reactive anthraquinone textile dyes under methanogenic conditions, *Water Res.*, 38 (2004) 1838–1852.
- [44] T. Kurbus, Y.M. Slokar, A.M. LeMarechal, The study of the effects of the variables on H<sub>2</sub>O<sub>2</sub>/UV decoloration of vinylsulphone dye: part II, *Dyes Pigm.*, 54 (2002) 67–78.
- [45] A. Nezamzadeh-Ejhieh, A. Shirzadi, Enhancement of the photocatalytic activity of ferrous oxide by doping onto the nano-clinoptilolite particles towards photodegradation of tetracycline, *Chemosphere*, 107 (2014) 136–144.
- [46] A. Nezamzadeh-Ejhieh, S. Hushmandrad, Solar photodecolorization of methylene blue by CuO/X zeolite as a heterogeneous catalyst, *Appl. Catal., A*, 388 (2010) 149–159.
- [47] A. Nezamzadeh-Ejhieh, M. Amiri, CuO supported Clinoptilolite towards solar photocatalytic degradation of p-aminophenol, *Powder Technol.*, 235 (2013) 279–288.
- [48] A. Nezamzadeh-Ejhieh, S. Khorsandi, Photocatalytic degradation of 4-nitrophenol with ZnO supported nano-clinoptilolite zeolite, *J. Ind. Eng. Chem.*, 20 (2014) 937–946.
- [49] M. Heidari-Chaleshtori, A. Nezamzadeh-Ejhieh, Clinoptilolite nano-particles modified with aspartic acid for removal of Cu (II) from aqueous solutions: isotherms and kinetic aspects, *New J. Chem.*, 39 (2015) 9396–9406.
- [50] C. Namasivayam, S. Sumithra, Removal of direct red 12B and methylene blue from water by adsorption onto Fe (III)/Cr (III) hydroxide, an industrial solid waste, *J. Environ. Manage.*, 74 (2005) 207–215.
- [51] V.K. Garg, M. Amita, R. Kumar, R. Gupta, Basic dye (methylene blue) removal from simulated wastewater by adsorption using Indian Rosewood sawdust: a timber industry waste, *Dyes Pigm.*, 63 (2004) 243–250.
- [52] A. Nezamzadeh-Ejhieh, M. Karimi-Shamsabadi, Comparison of photocatalytic efficiency of supported CuO onto micro and nano particles of zeolite X in photodecolorization of methylene blue and methyl orange aqueous mixture, *Appl. Catal., A*, 477 (2014) 83–92.
- [53] A. Nezamzadeh-Ejhieh, H. Zabihi-Mobarakeh, Heterogeneous photodecolorization of mixture of methylene blue and bromophenol blue using CuO-nano-clinoptilolite, *J. Ind. Eng. Chem.*, 20 (2014) 1421–1431.
- [54] N. Kannan, M.M. Sundaram, Kinetics and mechanism of removal of methylene blue by adsorption on various carbons—a comparative study, *Dyes Pigm.*, 51 (2001) 25–40.
- [55] R. Zeynolabedin, P. Moradihamedani, A. Bazayr, A. Marjani, Removal of methylene blue dye from aqueous solutions by elaeagnus gastifolia as an adsorbent, *Orient. J. Chem.*, 31 (2015) 271–276.
- [56] S. Pal, S. Ghorai, C. Das, S. Samrat, A. Ghosh, A.B. Panda, Carboxymethyl tamarind-g-poly (acrylamide)/silica: a high performance hybrid nanocomposite for adsorption of methylene blue dye, *Ind. Eng. Chem. Res.*, 51 (2012) 15546–15556.
- [57] K. Kalantari, M.B. Ahmad, H.R.F. Masoumi, K. Shameli, M. Basri, R. Khandanlou, Rapid and high capacity adsorption of heavy metals by Fe<sub>3</sub>O<sub>4</sub>/montmorillonite nanocomposite using response surface methodology: preparation, characterization, optimization, equilibrium isotherms, and adsorption kinetics study, *J. Taiwan Inst. Chem. Eng.*, 49 (2015) 192–198.
- [58] S.Z. Ali, M. Athar, M. Salman, M.I. Din, Simultaneous removal of Pb(II), Cd(II) and Cu(II) from aqueous solutions by adsorption on *Triticum aestivum* – a green approach, *Hydrol. Curr. Res.*, 2011 (2012) 1–8.
- [59] X.-J. Hu, Y.-G. Liu, H. Wang, A.-W. Chen, G.-M. Zeng, S.-M. Liu, Y.-M. Guo, X. Hu, T.-T. Li, Y.-Q. Wang, Removal of Cu (II) ions from aqueous solution using sulfonated magnetic graphene oxide composite, *Sep. Purif. Technol.*, 108 (2013) 189–195.
- [60] A. Nezamzadeh-Ejhieh, M. Kabiri-Samani, Effective removal of Ni (II) from aqueous solutions by modification of nano particles of clinoptilolite with dimethylglyoxime, *J. Hazard. Mater.*, 260 (2013) 339–349.

- [61] M. Anari-Anaraki, A. Nezamzadeh-Ejhieh, Modification of an Iranian clinoptilolite nano-particles by hexadecyltrimethyl ammonium cationic surfactant and dithizone for removal of Pb (II) from aqueous solution, *J. Colloid Interface Sci.*, 440 (2015) 272–281.
- [62] N. Danesh, M. Hosseini, M. Ghorbani, A. Marjani, Fabrication, characterization and physical properties of a novel magnetite graphene oxide/lauric acid nanoparticles modified by ethylenediaminetetraacetic acid and its applications as an adsorbent for the removal of Pb (II) ions, *Synth. Metals*, 220 (2016) 508–523.
- [63] N. Mao, L. Yang, G. Zhao, X. Li, Y. Li, Adsorption performance and mechanism of Cr (VI) using magnetic PS-EDTA resin from micro-polluted waters, *Chem. Eng. J.*, 200 (2012) 480–490.
- [64] M. Ciopec, C. Davidescu, A. Negrea, I. Grozav, L. Lupa, P. Negrea, A. Popa, Adsorption studies of Cr (III) ions from aqueous solutions by DEHPA impregnated onto Amberlite XAD7–Factorial design analysis, *Chem. Eng. Res. Design*, 90 (2012) 1660–1670.
- [65] Y.-S. Ho, Review of second-order models for adsorption systems, *J. Hazard. Mater.*, 136 (2006) 681–689.